

Published in final edited form as:

*J Neurochem.* 2012 July ; 122(2): 374–381. doi:10.1111/j.1471-4159.2012.07709.x.

## Microbiosensor for Alzheimer's Disease Diagnostics: Detection of Amyloid Beta Biomarkers

Shradha Prabhulkar<sup>1</sup>, Rudolph Piatyszek<sup>1</sup>, John R. Cirrito<sup>2</sup>, Ze-zhi Wu<sup>3</sup>, and Chen-Zhong Li<sup>1,\*</sup>

<sup>1</sup>Nanobioengineering/Bioelectronics Laboratory, Department of Biomedical Engineering, Florida International University, 10555 W Flagler Street, Miami, Florida

<sup>2</sup>Department of Neurology, Washington University, St. Louis

<sup>3</sup>Key Laboratory of Biorheological Science and Technology of the State Ministry of Education, College of Bioengineering, Chongqing University, China

### Abstract

Alzheimer's disease (AD) affects about 35.6 million people worldwide, and if current trends continue with no medical advancement, 1 in 85 people will be affected by 2050. Thus, there is an urgent need to develop a cost effective, easy to use, sensor platform to diagnose and study AD. The measurement of peptide amyloid beta (A $\beta$ ) found in cerebrospinal fluid (CSF) has been assessed as an avenue to diagnose and study the disease. The quantification of the ratio of A $\beta$ 1-40/42 (or A $\beta$  ratio) has been established as a reliable test to diagnose AD through human clinical trials. Therefore we have developed a multiplexed, implantable immunosensor to detect amyloid beta (A $\beta$ ) isoforms using triple barrel carbon fiber microelectrodes as the sensor platform. Antibodies act as the biorecognition element of the sensor and selectively capture and bind A $\beta$ 1-40 and A $\beta$ 1-42 to the electrode surface. Electrochemistry was used to measure the intrinsic oxidation signal of A $\beta$  at 0.65 V (vs Ag/AgCl), originating from a single tyrosine (Tyr) residue found at position 10 in its amino acid sequence. Using the proposed immunosensor A $\beta$ 1-40 and A $\beta$ 1-42 could be specifically detected in CSF from mice within a detection range of 20 nM to 50 nM and 20 nM to 140 nM respectively. The immunosensor enables real-time, highly sensitive detection of A $\beta$  and opens up the possibilities for diagnostic *ex-vivo* applications and research-based *in-vivo* studies.

### Introduction

AD is one of the most common neurodegenerative diseases currently affecting about 5.3 million people in the United States alone (Herbert et al., 2003). The national cost of caring for AD patients is ~ 100 billion each year. Despite important advances in the understanding of AD, much is still unknown about the underlying cause of the disease. A $\beta$  peptide comprising of 39–42 amino acids is the primary constituent of plaques found in the brain of patients suffering from AD. These insoluble plaques hinder the communication between neurons causing cell death, cognitive dysfunction, and behavioral abnormalities, they also initiate a host of other events including inflammation and tau aggregation as neurofibrillary tangles (Hardy and Higgins, 1992; Murphy and LeVine, 2010). However, till date there is no inexpensive, sensitive, real time detection strategy for monitoring A $\beta$  in-vivo and answer critical questions regarding its production, accumulation and clearance under physiological

\*Corresponding author: Prof Chenzhong Li, Department of Biomedical Engineering, Florida International University; licz@fiu.edu; Tel: (305) 348 0120 Fax: (305) 348 6954.

This paper is original and has no conflicts of interests to be reported.

and patho-physiological scenarios. The growing potential of the A $\beta$  ratio to act as a biomarker in diagnostic, prognostic, and therapeutics research studies warrants a better understanding of its biochemistry (Andreasen et al., 1999; Hampel et al., 2010; Blennow, 2004). There is still significant amount of research required to completely understand the link between A $\beta$  and the underlying cause of AD. Assessment of the interstitial and cerebrospinal pools of A $\beta$  may provide unique insights into the regulation of A $\beta$  aggregation and plaque formation (Bibl et al., 2007; Tampellini and Gunnar, 2010). Studies of this nature have been previously performed *in vitro* on neuronal cell cultures and brain slices using fluorescence microscopy and ELISA (Wyss-Coray et al., 2003). Towards in-vivo A $\beta$  measurements, microdialysis has been the most commonly utilized technique for the past 10 years (Cirrito et al., 2005).

This work has been directed towards the development of an electrochemical immunosensor capable of simultaneously detecting multiple A $\beta$  isoforms using the intrinsic electroactivity of A $\beta$  (Vestergaard et al., 2005). A $\beta$  contains a single Tyr residue at position 10, bearing a phenolic group, which is easily oxidized at the electrode surface (Chikae et al., 2008). Carbon fiber microelectrodes were used as the platform sensor as they offer advantages such as high signal to noise ratio, biological compatibility, and miniature size (Armstrong-James and Millar, 1979). Carbon based electrodes have been proven to sensitively detect Tyr oxidation (Okuno et al., 2007; Kerman et al., 2006). Using square wave voltammetry (SWV) the voltage applied to the carbon fiber microelectrode was scanned within a window of  $-0.2$  V to  $1.0$  V. The voltammogram shows increase/peak in measured current due to the oxidation of electroactive species, when the electrode attains their corresponding oxidation potential. When the electrode scans through  $0.6$  V, tyrosine residues present in A $\beta$  oxidize which causes up to 4 electrons/molecule to be released that are detected by the electrode as increased/peak current. While  $0.6$  V can cause oxidation of a variety of molecules, including all nearby tyrosines, an antibody covalently attached to the electrode surface can provide specificity for a particular target such as A $\beta$ . By monitoring the intrinsic electrochemical activities of A $\beta$ , direct, real-time, and reagentless detection is possible.

## Materials and Methods

### Materials

Carbon fibers ( $5\mu\text{m}$  in diameter) were donated by World Precision Instruments (Sarasota, FL). Borosilicate glass capillaries (3 barrels, inner diameter  $1.0$  mm) were obtained from Sutter Instrument Company (Novato, CA). Sylgard 184 was obtained from Dow Corning Corporation (Midland, MI). 1-ethyl-3-[3-dimethylaminopropyl] carbodiimide hydrochloride (EDC) and *N*-hydroxysulfosuccinimide (NHSS), EZ-Link Plus Activated Peroxidase was purchased from Thermo Fisher Scientific Inc. (Rockford, IL). A $\beta$  mouse monoclonal antibodies (mHJ2, mHJ7.4, mHJ5.1) were donated by Dr. Cirrito's laboratory. Antibodies mHJ2 and mHJ7.4 are C-terminal A $\beta_{40}$  and A $\beta_{42}$ -selective antibodies. Antibody mHJ5.1 recognizes the central domain of A $\beta$  (amino acids 17–28) and has no detectable cross-reactivity to other APP fragments as assessed by Western blot of brain tissue from APP transgenic mice. A $\beta_{1-40}$  and A $\beta_{1-42}$  synthetic peptide were obtained from American Peptide Company (Sunnyvale, CA). Mass spectrometric quality control of these peptides demonstrates 95% purity with no appreciable oxidation of the peptide, especially of the tyrosine amino acid at position 10. MES buffer, 3,3'-diaminobenzidine (DAB), hydrogen peroxide ( $\text{H}_2\text{O}_2$ ), sodium chloride, and other reagents were purchased from Sigma-Aldrich (St. Louis, MO).

## Instrumentation

Carbon fiber microelectrodes were prepared using P-97 Micropipette Puller and BV-10 Beveller acquired from Sutter Instrument Company (Novato, CA). Microelectrode activation and electrochemical measurements in connection with cyclic voltammetry (CV), differential pulse voltammetry (DPV) and square wave voltammetry (SWV) were carried out using the 600C Electrochemical Analyzer attached to a Picoamp Booster from CH Instruments, Inc. (Austin, TX). Scanning electron microscopy (SEM) of the triple barrel microelectrodes was carried out on the JEOL JSM 5900LV. Fluorescence microscopy was conducted using the IX81 from Olympus Inc. (Center Valley, PA). The cyclic square wave E-field applied was applied using the Leader LFG-13005 function generator and monitored using the Lafayette-82418 oscilloscope. A conventional three electrode cell consisting of an Ag/AgCl reference electrode (3 M KCl) (Bioanalytical Systems, IN, USA), and a platinum wire as an auxiliary electrode was employed.

## Fabrication of Triple Barrel A $\beta$ 1-40/A $\beta$ 1-42 Sensor

Triple barrel carbon fiber microelectrodes were fabricated using the same method as described in our previous work. Briefly, a single carbon fiber of diameter 5 $\mu$ m was attached to the stripped end of an insulated copper wire (diameter 0.2 mm) using a silver conductive paste. Each barrel of the borosilicate glass triple barrel capillary was then cannulated with a carbon fiber attached copper wire. The three copper wires were then fixed to the capillary using a fast drying epoxy resin. The capillary was then pulled using a micropipette puller. This pulling procedure results in two glass pipettes, one of which is discarded, and the other which holds three carbon fibers protruding from its tip. The junction between the carbon fibers and capillary is sealed with a drop of the Sylgard silicone preparation and allowed to cure until it becomes firm. The microelectrodes were then beveled at 45° using diamond abrasive plate, to obtain three disk shaped electrodes which are completely isolated from each other. The surface of the electrodes was cleaned by 5 s sonication in acetone, 1 M nitric acid, 1 M KOH and distilled water sequentially. To facilitate the binding of capture antibody, the microelectrodes were electroactivated using a 150 mM NaCl solution (pH=10) at 1.2V (vs. Ag/AgCl) for 8 minutes at room temperature. 0.4M of EDC and 0.1M of NHSS solutions in 0.1 M MES buffer (pH = 6) were then sequentially applied for 20 minutes to activate the carboxylic groups on the carbon fiber surface by forming a semi stable amine reactive NHS ester. The microelectrodes were then placed sequentially in mHJ2 (specific to A $\beta$ 1-40) (E1(40)), mHJ7.4 (specific to A $\beta$ 1-42) (E2(42)), and mHJ5.1 (specific to all isoforms of A $\beta$ ) (E3(TOT)) antibody solutions and a cyclic square wave E-field (-0.3 V to +0.3V, 0.1 Hz, 10 minutes) was applied sequentially to each electrode versus a platinum wire cathode. Application of the E-field allows for the selective placement of mHJ2 on E1, mHJ7.4 on E2(42) and mHJ5.1 on E3(TOT). Electrodes were incubated in 0.1 % ethanolamine solution to block any non-specific binding sites. In order to obtain quantitative measurements about the amount of antibody conjugated to the electrode, horseradish peroxidase (HRP) labeled antibodies were utilized. Labeling of A $\beta$  antibody (mHJ5.1) to HRP was performed as per protocol specified by Thermo Scientific. DAB and H<sub>2</sub>O<sub>2</sub> were used as the substrates in HRP catalysis reaction and measurements were conducted using DPV (Zhang et al., 2008). Crucial parameters related to efficient antibody immobilization such as antibody solution concentration, E-field parameters, and immobilization time were optimized based on the HRP based electrochemical results.

## Measurement of A $\beta$ 1-40 and A $\beta$ 1-42 in CSF solutions

The micro-immunosensors designed as aforementioned were then challenged using rat CSF solutions spiked with different combinations of A $\beta$ 1-40 and A $\beta$ 1-42 within a range of 10nM to 2 $\mu$ M. A cyclic square wave E-field (+ 0.75 to -0.75 V, 50 Hz, 10 minutes) was applied simultaneously to each of the three electrodes in order to accelerate the incubation process.

The electrodes were rinsed twice with PBS buffer (pH = 7.2) to get rid of any randomly or loosely attached A $\beta$  molecules. Square wave voltammetry (SWV) was used to simultaneously evaluate the response of each of the three microelectrodes before and after the immunoreactions. SWV voltammetry was performed using 10 mM PBS and 1 mM KCl as the supporting electrolyte.

### Measurement of A $\beta$ in CSF sample using ELISA

ELISA was performed on the samples used to challenge the immunosensors to take into account the amount of A $\beta$  lost due to sticking to plastic. To test the sensitivity of the A $\beta$  electrodes, human A $\beta$ 1-40 and human A $\beta$ 1-42 diluted in rat CSF. A $\beta$  was diluted and treated identically as those tests then quantified by sandwich ELISA to determine the exact concentration of each sample after electrodes were tested. A $\beta$  levels were assessed using sandwich ELISAs as described (Verges et al. 2011). Briefly, a mouse-anti-A $\beta$ 40 antibody (mHJ2) or mouse-anti-A $\beta$ 42 antibody (mHJ7.4) was used to capture and a biotinylated central domain antibody (mHJ5.1) was used to detect, followed by streptavidin-poly-HRP-40 (Fitzgerald Industries, Concord, MA). All ELISA assays were developed using Super Slow ELISA TMB (Sigma, St. Louis, MO) and absorbance read on a BioTek Epoch plate reader (Winooski, Vermont) at 650 nm. Though these ELISAs detect both human and rat A $\beta$ , rat A $\beta$  levels in the CSF were undetectable. The standard curves for each assay utilized either human A $\beta$ 1-40 or A $\beta$ 1-42 diluted fresh from concentrated stocks in formic acid.

### Statistical Analysis

All measurements were carried out in triplicate. All current responses recorded in this study were subtracted from the corresponding buffer current as the baseline unless specified otherwise. Results are expressed as mean value (standard deviation (SD) of three determinations, and statistical significance was defined at  $P < 0.05$ . The specificity and inter-assay reproducibility were determined with SPSS ver. 9.0 software using analysis of variance (ANOVA). The calibration curves for measurement of A $\beta$ 1-40 and A $\beta$ 1-42 were determined using correlation analysis.

## Results and Discussion

### Molecular architecture of the immunosensor

Here we report the development of a real-time immunosensor which can perform highly sensitive A $\beta$  measurements. The general molecular architecture and working principle of the immunosensor is shown in Scheme 1. To construct this immunosensor, 3 distinct antibodies were placed on each of the barrels of the carbon microelectrode. Antibodies mHJ2 placed on E1(40) and mHJ7.4 placed on E2(42) are highly specific to the detection of A $\beta$ 1-40 and A $\beta$ 1-42 respectively. Antibody mHJ5.1 which binds to the central region of the A $\beta$  peptide can capture all A $\beta$  isoforms and thus it act as a positive control for the immunosensor. The function of antibodies in the developed immunoensensor is three-fold. 1) Antibodies capture/ bind A $\beta$  molecules to the sensor surface which decreases the electron tunneling distance between the sensor surface and the A $\beta$  molecules. The decrease in the tunneling distance allows for electrons generated due to the oxidation of A $\beta$  to travel to the sensor surface during SWV and generate a current signal. Therefore lower quantities of A $\beta$  can also generate a measurable signal and improve sensor performance. 2) The capture/binding of A $\beta$  to the surface of the carbon fiber eliminates cross talk between the 3 microelectrodes during simultaneous measurements of A $\beta$ 1-40 and A $\beta$ 1-42. 3) Antibodies also enable highly specific detection of A $\beta$ 1-40 and A $\beta$ 1-42.

In this work square wave voltammetry for the oxidation of A $\beta$  was performed so that the magnitude of the resultant oxidation peak could be related to the amount of A $\beta$ 1-40/42 captured by the specific antibodies onto the electrode surface. Parameters involved in the preparation of an immunosensor play a vital role on its voltammetric response. Therefore the immunosensor was optimized for a maximum voltammetric response by optimizing key parameters such as amount of antibody immobilized on the electrode surface and incubation time. A cyclic square wave E-field was applied in order to accelerate the movement of antibodies towards the electrode surface which resulted in faster immobilization time.

### Characterization of fabricated triple-barrel carbon fiber microelectrodes

Carbon fiber microelectrodes have previously been employed for the direct electrochemical evaluation of neurotransmitters, enzymes, etc. In addition, the use of microelectrodes opens up the possibility of in-vivo application of the immunosensor. The miniaturized size of the electrode (several microns in diameter) would allow the careful selection of the biological matrix to be investigated with negligible physical damage to the implanted region (Huffman and Venton et al., 2008). Figure 2A shows the image of a triple barrel carbon fiber microelectrode obtained using SEM. The SEM image of the tip of the electrode shows three distinct disc shaped carbon fibers embedded in an epoxy matrix. From the SEM images each of the carbon fibers can be estimated to be 4–5  $\mu\text{m}$ . In order to precisely quantify the effective working area of each electrode, cyclic voltammetry was conducted. Based on Randles-Sevcik equation ( $I_{pa} = (2.69 \times 10^5) n^{3/2} AD^{1/2} \nu^{1/2} C_{red}$ ), the electroactive area (A) of all electrodes was determined from the anodic peak current ( $I_{pa}$ ) obtained in the cyclic voltammograms conducted using 0.03M  $\text{Fe}(\text{CN})_6^{-3/-4}$  ( $C_{red}$ ) at a specific scan rate ( $\nu$ ) as shown in Figure 1B. The diffusion co-efficient (D) was taken to be  $6.5 \times 10^{-6} \text{ cm}^2\text{s}^{-1}$  at 20  $^\circ\text{C}$  as derived by Kakuichi et al., 2002 and the average  $R_{eff}$  for the microelectrodes was calculated to be approximately  $\sim 5 \mu\text{m}$ .

### Optimization of antibody immobilization parameters

In the development of electrochemical immunosensors the immobilization of the bio-recognition element on the electrode is critical towards sensor performance. The surface of carbon fibers is well known to exhibit many reactive sites including hydroxylic, phenolic and carboxylic functionalities (Pantano and Kuhr, 1991). In order to expose these groups, the carbon fiber microelectrodes are electrochemically pretreated (Prabhulkar and Li, 2010). The microelectrodes were electroactivated using a 150mM NaCl solution (pH= 10) at 1.2 V (vs. Ag/AgCl) for 8 minutes at room temperature. The next step towards the construction of the immunosensor was to employ a carbodiimide reaction to selectively attach the three antibodies on the surface of each of the barrels of the microelectrode. In order to test binding of the antibody to the electrode surface, we first conjugated horseradish peroxidase (HRP) to the antibody. HRP provides a large oxidative signal that is easily detected by the electrode; HRP-labeled antibodies were only used to test for antibody absorption to the electrode. This involved the incubation of the pretreated microelectrodes in EDC and NHSS solutions. Initially the EDC and NHSS solutions were prepared in PBS buffer; however a negligible amount of antibody was bound to the electrode surface as measured by the electroactivity of the HRP label. We therefore switched the buffer to MES which showed a much higher peak from the HRP-labeled (mHJ5.1) antibodies as seen in Figure 3A.

HRP-labeled (mHJ.2) antibodies were used to optimize the parameters of the CSW E-field which was applied to accelerate the incubation process by promoting the transport of the antibodies to the electrode surface (Wei et al., 2009). The CSW E-field creates a mass transportation effect in the incubation solution which creates good mixing in shorter time as compared to diffusion kinetics. The voltage applied to three electrodes was varied from  $\pm 0.1$  V to  $\pm 0.5$  V for equal positive and negative cycles. The electrodes were monitored by

conducting DPV at every 1 minute interval for a period of 12 minutes. Based on the data shown in Figure 3B and 3C the optimum applied voltage and incubation time were chosen as  $\pm 0.3V$  and 7 minutes respectively. During the immobilization of antibodies on the immunosensor, only a fraction of the total antibody applied gets bound to the electrode surface. In order to conserve a precious resource such as anti-A $\beta$  antibodies, the optimal concentration was established empirically. In these experiments, an electrochemically activated and pretreated microelectrode was incubated in solutions ranging from 0.1 to 1.5  $\mu\text{g/ml}$  of mHJ5.1 antibody. The binding efficiency peaked and plateaued when more than 0.8  $\mu\text{g/ml}$  of mHJ5.1 antibody was applied as shown in Figure 3D. The low binding efficiency can be attributed to the presence of hydroxylic and phenolic groups in conjunction to the carboxylic groups which are not activated by EDC/NHSS and do not bind antibodies.

### Immunosensor Performance

After completing the optimization of key steps in the molecular architecture of the sensor, we assessed the ability of the immunosensor to simultaneously quantify A $\beta$ 1-40 and A $\beta$ 1-42 in CSF solutions using SWV with 10mM PBS and 1mM KCl as the supporting electrolyte. Figure 4 shows the voltammetric responses obtained after the incubation of four triple barrel microelectrodes with mouse CSF solutions containing 0 nM, 100 nM, 500 nM and 1 $\mu\text{M}$  A $\beta$ 1-40 and A $\beta$ 1-42 in equal concentrations. In each case when the potential was scanned between 0.0 to 0.8 V, a well-defined voltammogram consisting of an oxidation peak between 0.6 V to 0.65 V was obtained. The oxidation current was obtained almost instantaneously in our experiments with no delay needed for equilibrium. Further, no stringent temperature control was required during electrochemical evaluation. The signal obtained for E3(TOT) which acts as the control electrode was always higher as compared to the signals obtained for E1(40) and E2(42). The response obtained for E3(TOT) correlates with the activity of the mHJ5.1 antibody which recognizes most isoforms of A $\beta$  as it is targeted towards the central region of the peptide.

Linear calibration plots shown in Figure 5A and 5B were then constructed based on peak oxidation currents obtained vs. A $\beta$ 1-40 and A $\beta$ 1-42 concentrations respectively, in order to normalize the variations between electrodes. Based on the evaluation of the calibration plots the linearity of the immunosensor for the detection of A $\beta$ 1-40 and A $\beta$ 1-42 lies within the detection range of 20 nM to 50 nM and 20 nM to 140 nM respectively. The immunosensor demonstrates a sensitivity of 20 nM towards the detection of A $\beta$ 1-40 and A $\beta$ 1-42. The imprecision observed with the detection capabilities of the immunosensor towards A $\beta$ 1-40 and A $\beta$ 1-42 detection might be for several reasons: 1) related to the inherent immunoreaction kinetics of each antibody, 2) differential aggregation of A $\beta$  which could limit signal, 3) more non-specific absorption ("sticking") of A $\beta$ 1-42 versus A $\beta$ 1-40 to the apparatus.

Specificity is a crucial parameter which influences the performance of an immunosensor in real matrices, especially when an analyte at low concentrations needs to be detected in the presence of a much larger concentration of non-specific molecules. We need to prove that the presented sensor responds only to the A $\beta$  and anti-A $\beta$  immunoreaction and not to the nonspecific adsorption of other proteins. CSF contains free tyrosine and other proteins containing tyrosine amino acid residues which could cause false signaling. Ethanolamine which has been proven to be a successful blocking agent in previous studies (Frederix et al., 2004) was used to minimize these non-specific binding reactions.

In order to measure the specificity of each of the barrels towards a specific A $\beta$  isotope, three immunosensors were challenged using each of the following solutions 1) 1000 nM A $\beta$ 1-40 2) 1000 nM A $\beta$ 1-42 and 3) 500 nM A $\beta$ 1-40 and 500 nM A $\beta$ 1-42. SWV was performed before and after incubation of each microelectrode with analyte solution. Figure 5C shows

the average values of peak oxidation currents obtained after incubation from each of the barrel of three separate electrodes incubated in each of the above mentioned solutions. From the evaluation of Fig. 5C we can deduce that each of the barrels showed highly specific recognition properties. The signal obtained due to the non-specific adsorption of non-A $\beta$  proteins and non-corresponding A $\beta$  isoforms from each of the barrels was found to be minimum and statistically insignificant.

Since the electrochemical detection of Abeta is based on the electrochemical oxidation of Tyrosine group in Abeta, other electroactive groups, especially the Methionine 35 (Met35), located at residue 35 of A $\beta$ (1–42), might have interfere to the oxidation current of the Tyrosine group. Met is an easily oxidizable amino acid and can undergo 2-electron oxidation to form methionine sulfoxide (Schoneich, 2003). We compared the electrochemical oxidation potential of the two electrochemical active groups. We found that the oxidation of Tyr10 residue which occurs at a potential of 0.65 V (vs Ag/AgCl reference electrode), whereas the oxidation potential of zwitterionic Met35 at pH=7 is –0.057 V (vs Ag/AgCl reference electrode) (Brunelle and Rauk, 2004), which is much more negative than the oxidation potential of Tyr10. Therefore, in the present study the sweeping potential window for Abeta isoforms analysis was set up in the range from 0 to 0.8 V, in which the oxidization interference of Met35 on the electrochemical current of Tyr10 should be excluded.

Another consideration is regarded to the glycosylation of Tyr10, which could affect the electrochemical properties of Tyr10 leading to the miss interpretation of the electrochemical signal of Tyr10. The glycosylation of Tyr10 was commonly observed for shorter Abeta isoforms with sizes varying from Abeta 1–15, 1–16, 1–17, 1–18, 1–19, 1–20, 3–15, 4–15, 4–17, 5–17 (Halim, 2011). However, the most abundant isoforms of Abeta found in human CSF are with sizes from 1–38, 1–40, 1–42, which did not show glycosylation of Tyr10. The antibodies utilized in the immunosensor are specific towards the detection of Abeta-40 and Abeta-42 and do not show any significant cross-reactivity as observed from Figure 5C. Hence as Tyr10 present in Abeta 1-40 and Abeta 1-42 does not undergo glycosylation, it should not have any effect on the immunosensor response.

The stability of the microelectrodes with anti-A $\beta$  antibodies immobilized on their surface was evaluated over a period of one month. The micro immunosensors were stored in 0.1 M PBS solution at 4 °C after fabrication. The stability of the stored electrodes was studied by incubating them in freshly prepare solution containing 0.1 % BSA, 500 nM A $\beta$ 1-40, 500 nM A $\beta$ 1-42 in 0.1 M PBS at ph 7.2. The stability of the electrodes was evaluated by measuring their electrochemical response using square wave voltammetry. The electrochemical response of the microelectrodes progressively degraded after 4 days in storage. To test the inter-sensor reproducibility of the proposed system, three samples of different concentrations (100, 500 and 1000 nM) of A $\beta$ 1-40 and A $\beta$ 1-42 were tested first with different electrodes. The maximum value of the relative standard deviations was 14.2% ( $n = 3$ ) for inter-assay. This indicates that our detection strategy offers an acceptable reproducibility towards the detection of A $\beta$ 1-40 and A $\beta$ 1-42.

## Conclusion

In this work, a simple, sensitive and fast electrochemical multiplexed immunoassay for Alzheimer's disease biomarkers is presented. The current signal generated due to the oxidation of A $\beta$  was demonstrated to be feasible in the development of a direct, one-step biosensor. The reagentless detection process based on the inherent electroactivity of A $\beta$  greatly simplifies the sensor utilization. The incorporation of an electric field-driven strategy greatly shortened the sensor fabrication and sensor response time to 7 minutes which is a big

leap compared to the currently available ELISA methods which could take anywhere from 6 hours to several days in order to quantify A $\beta$ . The results show superior calibration curves, which enable the user to directly extrapolate the concentration of A $\beta$  found in a CSF sample based on the peak current obtained. Each of these single-use or non-recoverable microsensors show high specificity towards the detection of crucial A $\beta$  isoforms. The miniature size, reagent free detection capability and fast response of the immunosensor open up possibilities for its use in real-time in-vivo A $\beta$  detection.

## Acknowledgments

We thank AMERI (Advanced Material Engineering Research Institute, FIU) for technical support. This work has been also partially supported by the grant of NSF 1036579 (Lic), Chinese Ministry of Education 111 plan (B0623), National Institutes of Health K01 AG029524 (JRC) and P50 AG05681 (JRC) as well as the Charles F. and Joanne Knight ADRC at Washington University (JRC), and the Shmerler family (JRC).

## References

- Andreasen N, Hesse C, Davidsson P, Minthon L, Wallin A, Winblad B, Vanderstichele H, Vanmechelen E, Blennow K. Cerebrospinal fluid {beta}-amyloid (1-42) in Alzheimer disease: differences between early- and late-onset Alzheimer disease and stability during the course of disease. *Arch Neurol*. 1999; 56:673–680. [PubMed: 10369305]
- Armstrong-James M, Millar J. Carbon fibre microelectrodes. *J Neurosci Methods*. 1979; 1:279–287. [PubMed: 544972]
- Bibl M, Mollenhauer B, Lewczuk P, Esselmann H, Wolf S, Trenkwalder C, Otto M, Stiens G, Ruther E, Kornhuber J, Wiltfang J. Validation of amyloid- $\beta$  peptides in CSF diagnosis of neurodegenerative dementias. *Mol Psychiatry*. 2007; 12:671–680. [PubMed: 17339876]
- Blennow K. Cerebrospinal fluid protein biomarkers for Alzheimer's disease. *NeuroRx*. 2004; 1:213–225. [PubMed: 15717022]
- Brunelle P, Rauk A. One-Electron Oxidation of Methionine in Peptide Environments: The Effect of Three-Electron Bonding on the Reduction Potential of the Radical Cation. *J Phys Chem A*. 2004; 108:11032–11041.
- Chikae M, Fukuda T, Kerman K, Idegami K, Miura Y, Tamiya E. Amyloid- $\beta$  detection with saccharide immobilized gold nanoparticle on carbon electrode. *Bioelectrochemistry*. 2008; 74:118–123. [PubMed: 18676183]
- Cirrito JR, Yamada KA, Finn MB, Sloviter RS, Bales KR, May PC, Schoepp DD, Paul SM, Mennerick S, Holtzman DM. Synaptic activity regulates interstitial fluid amyloid- $\beta$  levels in vivo. *Neuron*. 2005; 48:913–922. [PubMed: 16364896]
- Cirrito JR, Kang JE, Lee J, Stewart FR, Verges DK, Silverio LM, Bu G, Mennerick S, Holtzman DM. Endocytosis Is Required for Synaptic Activity-Dependent Release of Amyloid- $\beta$  In Vivo. *Neuron*. 2008; 58:42–51. [PubMed: 18400162]
- Frederix F, Bonroy K, Reekmans G, Laureyn W, Campitelli A, Abramov MA, Dehaen W, Maes G. Reduced nonspecific adsorption on covalently immobilized protein surfaces using poly (ethylene oxide) containing blocking agents. *J Biochem Biophys Methods*. 2004; 58:67–74. [PubMed: 14597190]
- Hardy JA, Higgins GA. Alzheimer's disease: The amyloid cascade hypothesis. *Science*. 1992; 256:184–185. [PubMed: 1566067]
- Hempel H, Frank R, Broich K, Teipel SJ, Katz RG, Hardy J, Herholz K, Bokde ALW, Jessen F, Hoessler YC. Biomarkers for Alzheimer's disease: academic, industry and regulatory perspectives. *Nat Rev Drug Discov*. 2010; (7):560–574. [PubMed: 20592748]
- Hebert LE, Scherr PA, Bienias JL, Bennett DA, Evans DA. Alzheimer disease in the US population. *Arch Neurol*. 2003; 60:1119–1122. [PubMed: 12925369]
- Hilim A, Brinkmalm G, Ruetschi U, Westman-Brinkmalm A. Site-specific characterization of threonine, serine, and tyrosine glycosylations of amyloid precursor protein/amyloid beta-peptides in human cerebrospinal fluid. *Proc Natl Acad Sci U S A*. 2011; 108:11848–11853. [PubMed: 21712440]



- Huffman ML, Venton BJ. Carbon-fiber microelectrodes for in vivo applications. *Analyst*. 2008; 134:18–24. [PubMed: 19082168]
- Kakiuchi T, Usui H, Hobara D, Yamamoto M. Voltammetric properties of the reductive desorption of alkanethiol self-assembled monolayers from a metal surface. *Langmuir*. 2002; 18:5231–5238.
- Kerman K, Nagatani N, Chikae M, Yuhi T, Takamura Y, Tamiya E. Label-free electrochemical immunoassay for the detection of human chorionic gonadotropin hormone. *Anal Chem*. 2006; 78:5612–5616. [PubMed: 16878905]
- Kerman K, Vestergaard M, Chikae M, Yamamura S, Tamiya E. Label-free electrochemical detection of the phosphorylated and non-phosphorylated forms of peptides based on tyrosine oxidation. *Electrochem Commun*. 2007; 9:976–980.
- Murphy MP, LeVine H. Alzheimer's Disease and the Amyloid-Beta Peptide. *J Alzheimers Dis*. 2010; 19:311–323. [PubMed: 20061647]
- Okuno J, Maehashi K, Kerman K, Takamura Y, Matsumoto K, Tamiya E. Label-free immunosensor for prostate-specific antigen based on single-walled carbon nanotube array-modified microelectrodes. *Biosens Bioelectron*. 2007; 22:2377–2381. [PubMed: 17110096]
- Pantano P, Kuhr WG. Characterization of the chemical architecture of carbon-fiber microelectrodes. 1. Carboxylates. *Anal Chem*. 1991; 63:1413–1418. [PubMed: 1928721]
- Prabhulkar S, Li CZ. Assessment of oxidative DNA damage and repair at single cellular level via real-time monitoring of 8-OHdG biomarker. *Biosens Bioelectron*. 2010; 26:1743–1749. [PubMed: 20863679]
- Schöneich C, Pogocki D, Hug GL, Bobrowski K. Free radical reactions of methionine in peptides: mechanisms relevant to beta-amyloid oxidation and Alzheimer's disease. *J Am Chem Soc*. 2003; 125:13700–13713. [PubMed: 14599209]
- Tampellini D, Gouras GK. Synapses, Synaptic Activity and Intraneuronal A in Alzheimer's Disease. *Front Aging Neurosci*. 2010; 2 pii-13.
- Verges D, Restivo J, Goebel W, Holtzman D, Cirrito J. Opposing synaptic regulation of amyloid- $\beta$  metabolism by NMDA receptors in vivo. *J Neurosci*. 2011 In press.
- Vestergaard M, Kerman K, Saito M, Nagatani N, Takamura Y, Tamiya E. A rapid label-free electrochemical detection and kinetic study of Alzheimer's amyloid beta aggregation. *J Am Chem Soc*. 2005; 127:11892–11893. [PubMed: 16117499]
- Wei F, Patel P, Liao W, Chaudhry K, Zhang L, Arellano-Garcia M, Hu S, Elashoff D, Zhou H, Shukla S. Electrochemical sensor for multiplex biomarkers detection. *Clin Cancer Res*. 2009; 15:4446–4452. [PubMed: 19509137]
- Wyss-Coray T, Loike JD, Brionne TC, Lu E, Anankov R, Yan F, Silverstein SC, Husemann J. Adult mouse astrocytes degrade amyloid- in vitro and in situ. *Nat Med*. 2003; 9:453–457. [PubMed: 12612547]
- Zhang S, Yang J, Lin J. 3, 3'-diaminobenzidine (DAB)-H<sub>2</sub>O<sub>2</sub>-HRP voltammetric enzyme-linked immunoassay for the detection of carcinoembryonic antigen. *Bioelectrochemistry*. 2008; 72:47–52. [PubMed: 18248855]

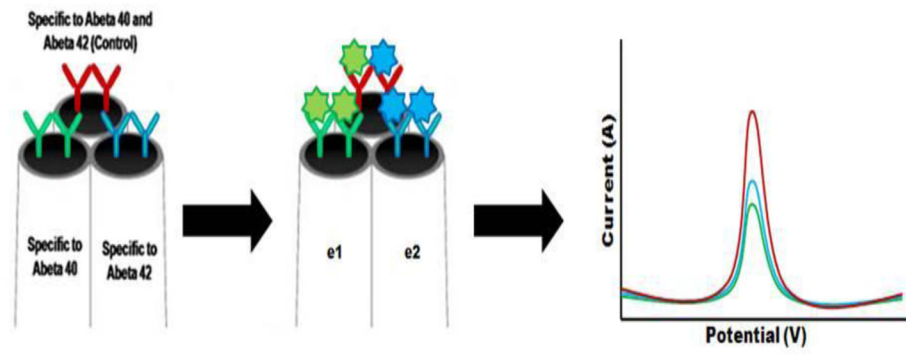


**Figure 1.** Schematic illustration of the microbioelectronic detection system for Alzheimer's disease related A $\beta$ 1-40 and A $\beta$ 1-42 peptides.

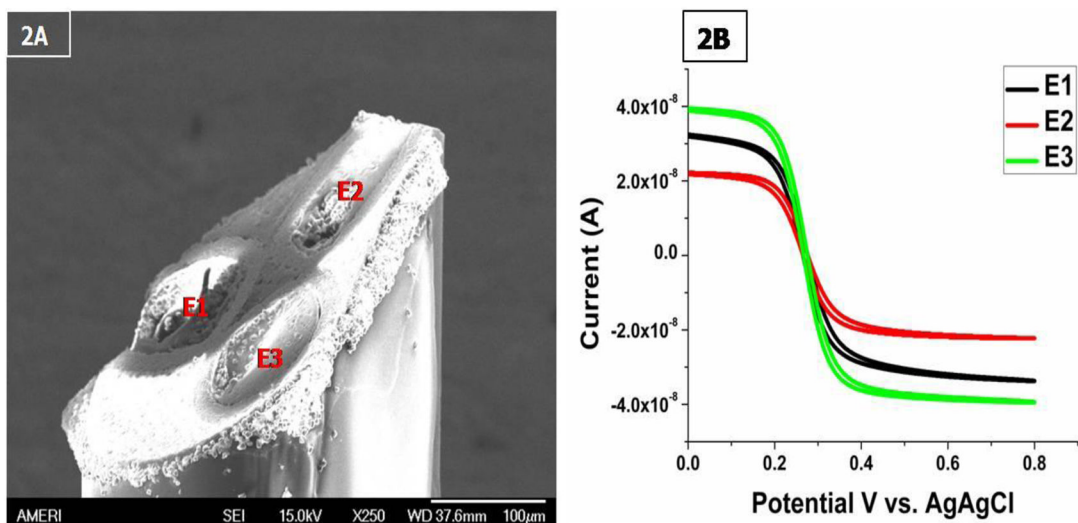


**Figure 2.** (A) SEM image triple barrel carbon fiber microelectrode. (B) Cyclic voltammograms of the three barrels of a microelectrode. Measurements were taken in 0.03 mol/L potassium ferricyanide solution. Scan rate was 0.1 V/s and potential limits were from 0.0 to +0.8 V versus Ag/AgCl reference electrode.

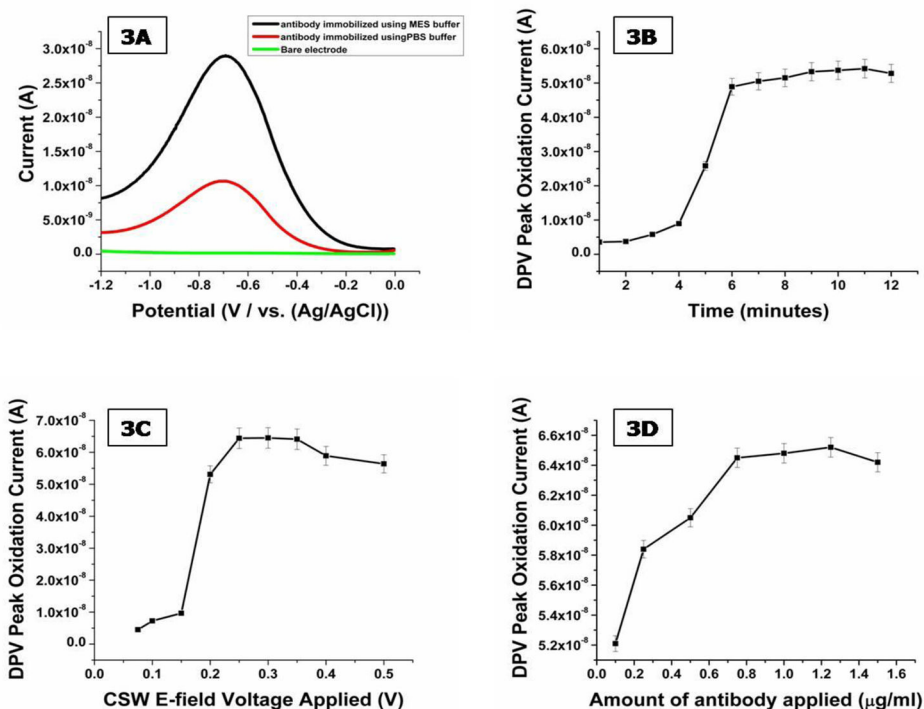


**Figure 3.**

(A) DPV response obtained from HRP labeled antibodies immobilized using PBS and MES buffer solutions. (B) Bare triple barrel carbon fiber microelectrode incubated with a 1.5 µg/ml solution of HRP labeled anti-A $\beta$  antibody (mHJ5.1) solution. DPV was every 1 minute performed using 10 mM PBS buffer and 1 mM KCl as supporting electrolyte. Oxidation peak current is plotted versus responding incubation time. (C) Effects of driving potential on the amount of antibody immobilized on electrode surface using 1000 µg/ml antibody solution and incubation time of 7 minutes. (D) HRP signal generated by electrode following the application of an increasing load of HRP labeled antibody.

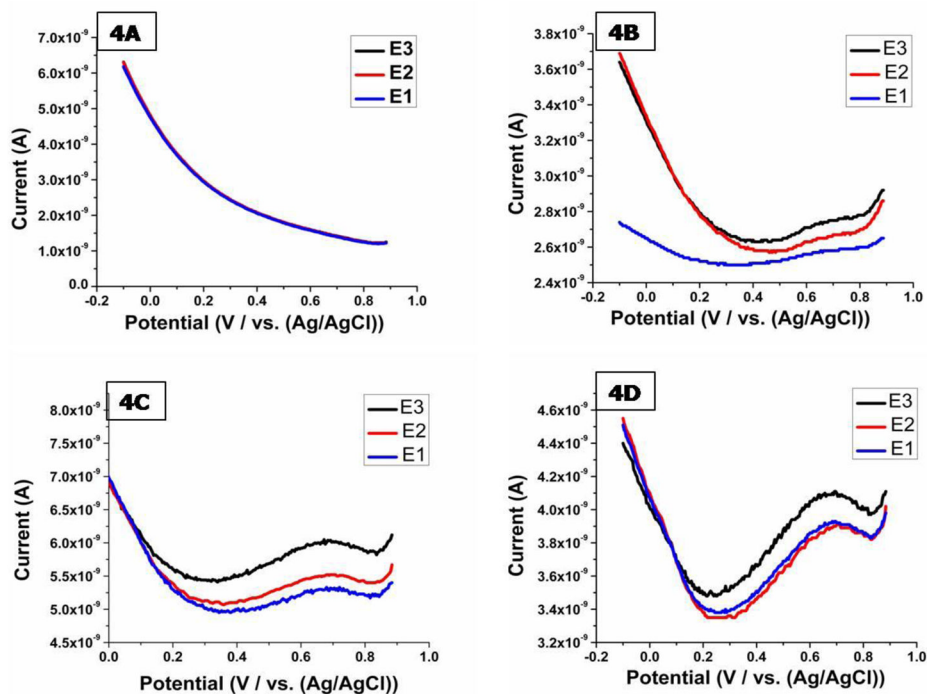


**Figure 4.** Square wave voltammetric responses of 3 barrel of the immunosensor obtained in rat (A) cerebrospinal fluid solution, spiked with (B) 100 nM  $A\beta$ 1-40 and 100 nM  $A\beta$ 1-42 (C) 500 nM  $A\beta$ 1-40 and 500 nM  $A\beta$ 1-42 (D)  $1 \mu\text{M}$   $A\beta$ 1-40 and  $1 \mu\text{M}$   $A\beta$ 1-42 solutions. Square wave voltammetry parameters: Init E (V) =1; Final E (V) =0; Incr E (V)= 0.004; Amplitude (V) = 0.04; Frequency (Hz) = 500.

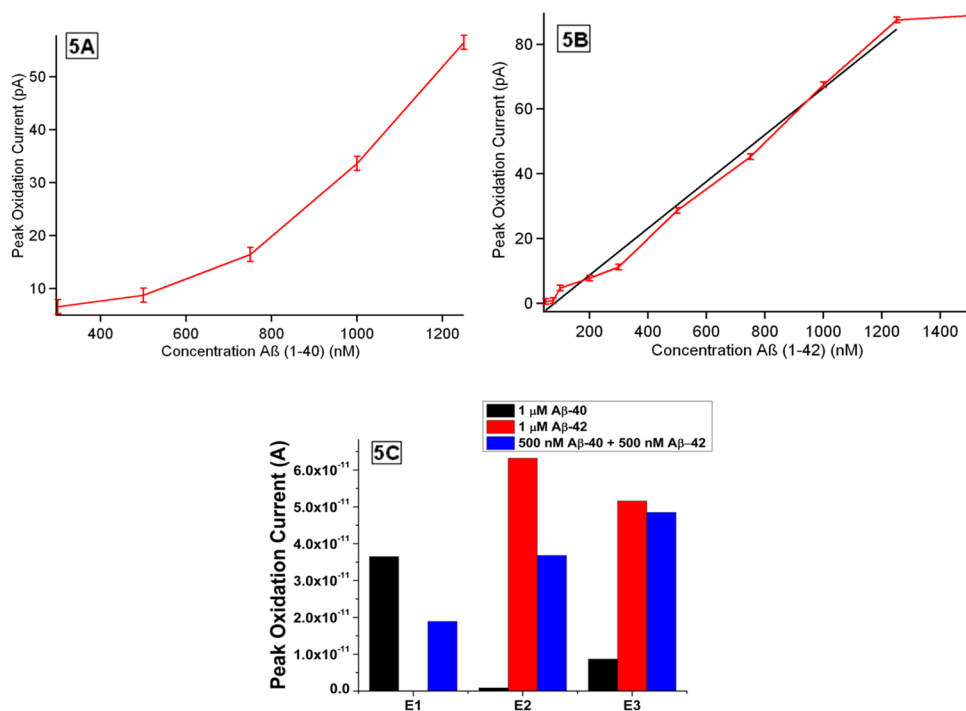


**Figure 5.** (A) Calibration curve: the linear relationship between peak oxidation current and Aβ1-40 concentration. (B) Calibration curve: the linear relationship between peak oxidation current and Aβ1-42 concentration. (C) Oxidation peak current obtained from three anti-Aβ modified carbon fiber microelectrodes after being incubated with 1 μM of Aβ1-40, 1 μM of Aβ1-42 and 500 nM of Aβ1-40 + 500 nM of Aβ1-42 spiked into rat cerebrospinal fluid solutions respectively. Measurements were performed in 10 mM PBS buffer and 1mM KCl versus Ag/AgCl.